



Fate and biological effects of silver, titanium dioxide, and C₆₀ (fullerene) nanomaterials during simulated wastewater treatment processes

Yifei Wang^{a,1}, Paul Westerhoff^{a,*}, Kiril D. Hristovski^b

^a School of Sustainable Engineering and the Built Environment, Arizona State University, PO Box 5306, Tempe, AZ 85287-5306, United States

^b Department of Technology Management, College of Technology and Innovation, Arizona State University, 6075 S. Williams Campus Loop W, Mesa, AZ 85212, United States

ARTICLE INFO

Article history:

Received 24 June 2011

Received in revised form

15 September 2011

Accepted 30 October 2011

Available online 7 November 2011

Keywords:

Nanomaterials

Wastewater

Titanium dioxide

Fullerenes

Biosolids

ABSTRACT

As engineered nanomaterials (NMs) become used in industry and commerce their loading to sewage will increase. In this research, sequencing batch reactors (SBRs) were operated with hydraulic (HRT) and sludge (SRT) retention times representative of full-scale biological WWTPs for several weeks. Under environmentally relevant NM loadings and biomass concentrations, NMs had negligible effects on ability of the wastewater bacteria to biodegrade organic material, as measured by chemical oxygen demand (COD). Carboxy-terminated polymer coated silver nanoparticles (*fn*-Ag) were removed less effectively (88% removal) than hydroxylated fullerenes (fullerols; >90% removal), nano TiO₂ (>95% removal) or aqueous fullerenes (*n*C₆₀; >95% removal). Experiments conducted over 4 months with daily loadings of *n*C₆₀ showed that *n*C₆₀ removal from solution depends on the biomass concentration. Under conditions representative of most suspended growth biological WWTPs (e.g., activated sludge), most of the NMs will accumulate in biosolids rather than in liquid effluent discharged to surface waters. Significant fractions of *fn*-Ag were associated with colloidal material which suggests that efficient particle separation processes (sedimentation or filtration) could further improve removal of NM from effluent.

© 2011 Elsevier B.V. All rights reserved.

1. Introduction

The use of nanomaterials (NMs) in commercial products is rapidly increasing. In 2006, more than 300 commercial products on the market claimed to have enhanced properties due to incorporated NMs; this number had more than quadrupled by 2010 [1,2]. Silver is the most common NM used in products, followed by carbon-based NMs and TiO₂ [2]. As a result of this increasing production and utilization, research has begun to assess the potential risks related to the presence of these ultra-small materials in the environment, including effects on bacteria, algae, fish, and other organisms [1,3–13]. Risk assessment and management rely upon both effects data (e.g., toxicity) and exposure information. Therefore, both to assess the risk of engineered NMs in the environment and to control their release, an understanding of the processes that affect NM flux through society is critical. This has been the focus of recent exposure modeling assessments [14–19].

Many NMs used in commercial products will enter municipal or industrial wastewaters, which are collected and treated at centralized wastewater treatment plants (WWTPs) [19–22]. Although NMs may undergo transformation (e.g., dissolution of metal ions from metal-based NMs), the primary process of NM removal from sewage will be association with biosolids, a process termed biosorption, and their subsequent removal by sedimentation and/or filtration [21,23–25]. Field studies discovered silver sulfide nanoparticles generated during the wastewater treatment process, which indicates the role of WWTPs in the transformation of silver NMs [26]. NMs in biosolids are often land applied such that terrestrial organisms are exposed. NMs that are not removed pass through the WWTPs in the water and are discharged into rivers, lakes, and oceans, where aquatic organisms are exposed [21,27].

The objectives of this study were (1) to quantify the removal efficiency of silver, titanium dioxide, and carbonaceous NMs from simulated wastewater and into biosolids using lab-scale sequencing batch reactors (SBRs) and (2) to evaluate the effects of NMs on the function of bacteria in WWTPs. By accomplishing these goals, we can develop a better understanding of the fate of these NMs in WWTPs. Previous studies on NM fate during wastewater treatment have used static batch reactors or predictive life-cycle models [17,28–30]. Here we operate SBRs for extended periods of time with continuous daily loadings of NMs along with removal of settled effluent and settled biosolids.

* Corresponding author. Tel.: +1 480 965 2885; fax: +1 480 965 0557.

E-mail addresses: ywang187@asu.edu (Y. Wang), p.westerhoff@asu.edu (P. Westerhoff), kiril.hristovski@asu.edu (K.D. Hristovski).

¹ Tel.: +1 480 284 9348; fax: +1 480 965 0557.

² Tel.: +1 480 727 1291; fax: +1 480 727 1684.

2. Experimental approach

2.1. Sequencing batch reactors

Laboratory-scale sequencing batch reactors were used in the experiments. For most experiments the reactors had a liquid volume of 1.6 L (Fig. SI.1A and B provides details); only for a long-term test (150 days) was a slightly different configuration used (Fig. SI.1C). The long-term experiments were conducted to vary nC_{60} feed concentrations and biomass levels within a continuously operated system. Samples were aerated and mechanically mixed. The reactors were seeded with bacteria culture (return activated sludge) from Northwest Wastewater Treatment Plant in Mesa, Arizona which operated with a sludge retention time close to six days. The reactors were supplied with a previously published synthetic feed solution [31] (detailed composition provided in SI) comprised of salts, trace nutrients, buffer and monosodium glutamate ($C_5H_8NO_4Na$) as a carbon and nitrogen source. This feed solution had a conductivity of 0.5 mS, COD of 780 mg/L, and total dissolved nitrogen (TDN) of 150 mg N/L. Nanomaterials were added to the feed solution, which was then added to the SBR. Detailed operation and sampling procedures are presented in the Supplemental Information (SI). Briefly, the hydraulic residence time (HRT) of the SBRs was 8 h (aeration time) plus settling. The sludge retention time (SRT) was managed in most test at 6.4 days, which is typical for activated sludge systems for COD removal; only in lower TSS tests for the 150-day fullerene tests was the SRT decreased to 4.4 days which was necessary to maintain the lower target TSS level. HRT and SRT were regulated by removing settled supernatant and mixed suspended solids. Typical wastewater treatment systems operate at TSS levels of 1500–2500 mg/L, and this was the target level for most experiments. Lower TSS levels were targeted during the 150 day SBR experiment to demonstrate in continuous flow operation the effect of biomass levels on nanomaterial removal. Reactors were operated for several weeks to reach steady state, which was determined on the basis of consistent total suspended solids (TSS) concentration and effluent chemical oxygen demand (COD), before addition of NMs began. Control reactors were operated with (1) the feed solution with NMs but no biomass and (2) the feed solution with no NMs.

2.2. Preparation of nanomaterial stock suspensions

Stock suspensions of NMs were prepared using ultrapure water (Milipore Milli-Q) with conductivity <1.1 $\mu S/cm$. Characteristics of the NMs in the stock suspensions are summarized in Table 1 and Fig. SI.2. The stock solution of functionalized (carboxyl terminated polymer coating) silver nanoparticles ($fn-Ag$) used the as-received liquid solution (~ 300 mgAg/L) from the manufacturer (Northern Nanotechnologies, Ontario, Canada). The $fn-Ag$ stock solution contained 8–10% ionic silver as measured by ion-specific electrode (ISE) (Accumet[®] Silver/Sulfide, Fisher), which was used in combination with a pH/mV meter (Φ^{TM} 250 series, Beckman) to measure free Ag^+ ions, and confirmed by centrifugal ultrafiltration using a 10 kDa membrane (Amicon). To investigate the potential toxic effects of ionic silver, stock solutions were prepared by dissolving 200 mg Ag from $AgClO_4$ (Sigma–Aldrich) in 1 L of ultrapure water.

Titanium dioxide NM stock suspensions were prepared using Hombikat TiO_2 powder (Sachtleben Chemie GmbH, Duisburg, Germany). Hombikat TiO_2 has a low iso-electric point ($pH_{ZPC} \sim 5.3$ as estimated using a ZetaPALS instrument, Brookhaven Instruments, NY). The stock suspension was prepared by suspending 1 g of TiO_2 into 1 L of ultrapure water and sonicating it with an ultrasonic probe (5T Standard Probe, Model 2000U, Ultrasonic Power Cooperation, Freeport, IL, USA) for 2 h at 200 W/L. Portions of the suspension were centrifuged at $1000 \times g$ for 30 min, and the

supernatant was used as the stock TiO_2 suspension ($n-TiO_2$). The stock solution contained 320 mgTi/L. XRD results indicate that all TiO_2 is pure anatase (Fig. SI.2). Suwannee River natural organic matter (NOM) (International Humic Substances Society) was added during select experiments.

Fullerene (C_{60}) and hydroxylated-fullerene ($C_{60}(OH)_{24-y}Na_y$) were purchased from MER Corporation, Tucson, Arizona. Aqueous fullerene (nC_{60}) was prepared by adding ~ 500 mg of C_{60} dry powder to 1 L nanopure water and sonicating at 200 W/L for 6 h. The solution was then filtered (Whatman GFF) and permeate became the stock solution. The fullerol stock solution was prepared similarly by adding ~ 70 mg of $n-C_{60}(OH)_{24-y}Na_y$ to 500 mL ultrapure water, sonicating for 30 min, and then filtering.

2.3. Analytical methods

Organic carbon substrate utilization by the biomass was assessed using COD, which was measured via the closed reflux dichromate colorimetric method 5220 D (Standard Methods for Water and Wastewater Analysis) [32]. Sample pH was also measured (Beckman $\Phi 250$ pH/Temp/mV Meter, Beckman Coulter Inc., Fullerton, CA, USA). Dissolved organic carbon (DOC) and total organic carbon (TOC) concentrations were analyzed using a TOC instrument (Shimadzu TOC-V CSH). Biomass concentration was determined as the TSS concentration following the Standard Methods for Water and Wastewater Analysis [32].

Metal concentrations in liquid samples were determined by acid digestion followed by analysis using Inductively Coupled Plasma-Optical Emission Spectroscopy (ICP-OES) (Thermo iCAP6300 ICP-Optical Emission Spectrometer). Detection limits were below 1 $\mu g/L$. Liquid aliquots of silver nanoparticle dispersions were digested in concentrated ultrapure nitric acid with addition of 30% H_2O_2 using a hotplate digestion method [32]. Liquid aliquots of titanium dioxide nanoparticle dispersions were converted to titanium ions by digestion in a mixture of ultrapure concentrated nitric and sulfuric acids at $T > 220^\circ C$ using a hotplate digestion method [32]. Recovery of metals from nanoparticle was between 90% and 110%, within acceptable USEPA ranges. Metal concentrations in dry biomass samples were determined by filtering (Whatman GF/F filter) and drying the biomass at $105^\circ C$ to constant mass prior to acid digestion. Dry biomass was digested following USEPA SW-846, Method 3050B [32].

Concentrations of fullerenes and fullerols were analyzed using a UV/VIS spectrophotometer (HACH DR5000) at 347 nm and 400 nm, respectively, during short-term SBR tests. During long-term SBR tests (150 days) using fullerenes, nC_{60} was measured after liquid–liquid extraction (10 mL sample, 30 mL glacial acetic acid to prevent emulsion formation, 10 mL toluene) followed by LC/MS (Days 0–45) and then HPLC (Days 45–150) following established methods [33–35]; comparable results for the two methods obtained between Days 30 and 60 validated the switch to the easier HPLC method. Both methods had detection limits of 1 $\mu g/L$ when the toluene extract was reduced to 0.5 mL prior to analysis.

Scanning electron microscopy/focused ion beam microscopy equipped with an energy dispersive X-ray microanalysis system (SEM/EDS) (FEI Nova 200 SEM/FIB with EDAX) and transmission electron microscopy (TEM) equipped with EDS (Philips CM200 FEG TEM/STEM with EDAX) was used to characterize the nanoparticles visually and determine their presence in the biomass. Zeta potential and particle sizes were estimated using the phase analysis light scattering technique (PALS) (ZetaPALS Brookhaven Instruments, Brookhaven, NY) on nanomaterials in the feed solution matrix. PALS particle sizes were estimated using the monomodal size distribution (MSD). X-ray diffraction (Siemens D5000, CuK_{α} X-ray source) was used to characterize the crystallographic structure of NMs.

Table 1
Summary of nanomaterial properties.

Nanomaterial	Supplier	Concentration applied to SBR (mg/L)	DLS mean diameter (nm)		Zeta potential at pH 7 (mV) ^a
			In nanopure water (polydispersity)	In SBR feed solution	
<i>fn</i> -Ag	Northern Nanotech (Vive Nano)	0.5–1.5	~5 (0.322)	~30	–6
<i>n</i> -TiO ₂	Hombikat	0.5–2.0	~20 (0.233)	~1700	–30
Ag- <i>n</i> C ₆₀	MER Corp.	0.5–2.5	~88 (0.172)	~129	–52
<i>n</i> -C ₆₀ (OH) _{<i>x</i>} (ONa) _{<i>y</i>}	MER Corp.	2.5	~40 (0.128)	~90	–21

^a Measured in the SBR feed solution.

3. Results and discussion

3.1. Influence of nanomaterials on substrate utilization and bacterial growth

NM dosages of 0.5–2.5 mg/L were applied to SBRs, which were operated for several weeks (Table 1). Organic carbon substrate utilization by the bacterial biomass was assessed by analyzing COD in the effluent. Over a 27-day operation period, influent COD levels in the feed solution averaged 748 ± 13 mg/L. The average COD level of the settled effluent from SBRs without NMs was 64 ± 28 mg/L. The average (27-day operation) COD in the settled effluent from SBRs with *fn*-Ag and *n*-TiO₂ were 45 ± 12 mg/L and 45 ± 16 mg/L, respectively. SBRs supplied with ionic silver (AgClO₄) had an average COD in the settled effluent of 39 ± 19 mg/L. Effluent COD from the SBRs with fullerene and fullerol were 21 ± 8 mg/L and 32 ± 12 mg/L, respectively. Plots of COD in SBR settled effluents are presented in Fig. SI.3. Based on an *F*-test, effluent COD levels in SBRs with and without NMs were not statistically different ($p > 0.07$). Thus in our study, under the TSS levels (see below) and NM dosages reflective of the upper limit of expected environmental concentrations, the presence of NMs did not adversely affect COD removal in the biological reactors.

To further confirm that NMs had minimal impact on COD removal, COD removal kinetics were evaluated during individual loading cycles. For example, in a control SBR without NMs, COD levels rapidly decreased from 804 mg/L to less than 35 mg/L within 2 h and then remained relatively constant for the duration of the loading cycle (Fig. SI.4). The pseudo first-order rate constant for the loss of COD over the first two hours of the cycle was approximately 1.5 h^{-1} , and was not different in the presence or absence of NMs. The only exception occurred with an initial addition of fullerol, as approximately 6 h were required to achieve the effluent COD level on the first day of fullerol addition. This slower COD removal disappeared during subsequent operational cycles, suggesting the bacteria may have adapted (for COD removal) to the presence of fullerol. Although the antimicrobial activity of silver nanoparticles and silver ions exists [36,37], the functional redundancy of the microbial community may have ensured that the biomass removed COD when the systems operated at a TSS value similar to that of a full-scale activated sludge process.

The biomass concentration, measured as TSS, was relatively constant for most SBR experiments (Fig. SI.5). Fullerene and fullerol addition resulted in similar TSS levels as the controls and exhibited no long-term detrimental influence on COD removal. Biomass concentrations were also constant with *n*-TiO₂ (average 1.3 ± 0.2 gTSS/L). Biomass concentrations were similar to controls for *fn*-Ag (average 1.8 ± 0.2 gTSS/L) and AgClO₄ (average 1.7 ± 0.2 gTSS/L), except during the first operational cycle of feed solutions containing NMs was a significant change (10–15% decline) in TSS observed. This could suggest an initial shock from the NMs, or silver ions, after which the mixed microbial community adapted to their presence.

3.2. Nanomaterial removal from the liquid phase in sequencing batch reactors

3.2.1. Nanomaterial removal without biomass

The *fn*-Ag was not removed in absence of biomass (control) experiments (Fig. 1), as the influent and settled effluent silver concentrations were comparable. Fullerol was also stable in the feed solution and was not removed during the operation of SBRs without biomass (data not shown). In contrast, in control tests approximately 70% of the nano-scale titanium dioxide (*n*-TiO₂) was removed during each SBR loading cycle (Fig. 2). Removal of *n*-TiO₂ without biomass present was presumably due to aggregation and sedimentation (abiotic mechanisms) caused by the modest ionic strength present in the feed solution and the time permitted for settling prior to removal of the supernatant at the end of each SBR cycle (i.e., settled effluent). When the *n*-TiO₂ was added into the feed solution, the nanoparticles rapidly aggregated and formed large particles (>1 μm). In an attempt to stabilize *n*-TiO₂ in the control reactors, 5 mgDOC/L of NOM was fed with *n*-TiO₂. The NOM concentration of 5 mg/L was selected based upon previous work which should significant stabilization of *n*-TiO₂ in the presence of 0.5–10 mg/L of NOM [38]. Most wastewater effluents contain 4–15 mg/L of DOC. However, NOM had minimal effect on *n*-TiO₂ removal, presumably because divalent cations (Mg²⁺ and Ca²⁺) present in our feed solution still complexed with the NOM coatings on the NMs and facilitated their aggregation [38].

Fullerenes were stable in the feed solution during operation of the SBR without biomass for 3 days. After that, the average colloid diameter measured by DLS increased from 129 nm to 632 nm, and the concentration decreased (Fig. SI.6a). We speculated that the cause was bacterial growth in the feed solution even though no biomass was added. Therefore, another SBR was started with feed solution containing fullerenes as well as a biocide (100 mg/L of sodium azide). Fullerenes remained stable in this feed solution (i.e., no removal caused by aggregation and sedimentation) (Fig. SI.6b).

3.2.2. NM removal in the presence of biomass

NMs were loaded with each new feed solution addition at the beginning of each operational cycle (feed solution addition, mixed aeration, withdrawal of mixed suspended solids for SRT management, settling, withdrawal of settled supernatant for HRT management, replenishment with fresh feed solution containing NMs) for a fixed duration to study NM removal, and then the reactors operated with replenishment of the feed solution only (no NMs added) to evaluate “washout” from the reactor. Fig. 1 shows influent and effluent silver data for *fn*-Ag in reactors both with and without biomass added. In the presence of biomass (1.8 ± 0.2 gTSS/L; Fig. SI.5) after reaching steady state, $88 \pm 4\%$ of the *fn*-Ag was removed from settled supernatant (i.e., effluent) when fresh NMs and feed solution were added during each operational cycle (Days 1–18). After Day 18, replenishment of the feed solution without NMs continued (i.e., zero silver in the SBR influent). Effluent silver concentrations took an additional few days to reach influent

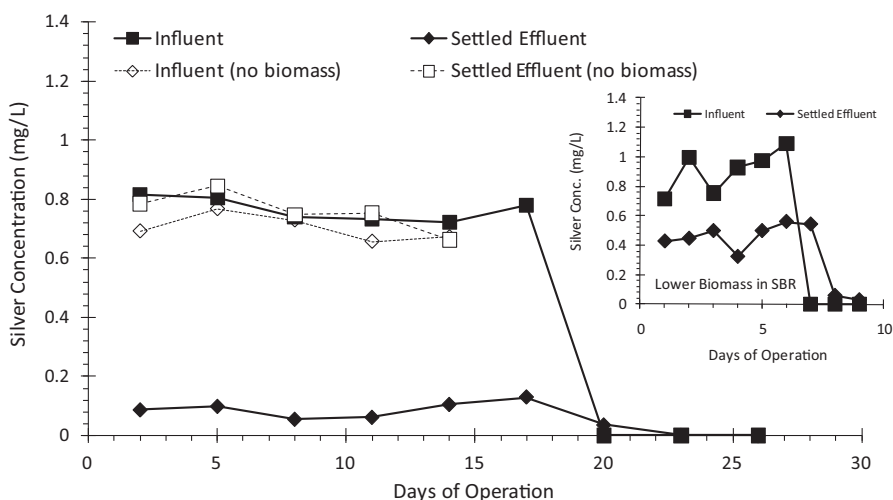


Fig. 1. Silver concentrations in SBRs either without biomass (open symbols) or with biomass (solid symbols; biomass concentration ranged from 2 to 2.5 mgTSS/L). Inset shows lower silver removal results for shorter term (9-day) experiments (biomass concentration ranged from 1.2 to 1.5 mgTSS/L).

levels, which indicates a slow “washout” of silver after ceasing *fn*-Ag addition into the SBR (feed water without NMs was added after Day 18). Operation of a 9-day SBR test at a lower biomass concentration (1.1 ± 0.2 mgTSS/L) resulted in $49 \pm 10\%$ removal of silver while *fn*-Ag was added (Fig. 1 inset). Again, after cessation of *fn*-Ag addition on Day 7, a short washout period of silver from the reactor was observed.

Another SBR was then operated for 30 days with an average influent *fn*-Ag concentration of 2.0 ± 0.1 mg/L and a TSS of 0.55 ± 0.1 gSS/L (Fig. SI.7). The settled supernatant was sampled directly as well as filtered using 0.45- μ m membranes and 10 kDa centrifugal ultrafiltration membranes. During this period the silver removal in the settled, 0.45- μ m membrane-filtered, and 10 kDa membrane-filtered effluent averaged $58 \pm 18\%$, $88 \pm 15\%$, and $99 \pm 0.1\%$, respectively; the filtered effluent always had a larger removal than the settled effluent. Therefore, a fraction of the silver was associated with colloidal cellular material (i.e., between 0.45 μ m and 10 kDa) that did not completely settle during the cyclic operation (i.e., it was present in the supernatant). In separate experiments using the stock solution, the 10 kDa membranes retained *fn*-Ag and allowed ionic silver to pass through. Thus ionic silver was

concluded not to be present in the SBR effluent. Ionic silver could have precipitated as silver chloride or silver sulfide, or sorbed onto biomass. TEM analysis was conducted on silver nanoparticles in the settled biosolids (Fig. SI.8). The size and shape of the silver in the biosolids were consistent with the initial *fn*-Ag nanoparticles, and EDX confirmed them as silver. Therefore, a significant portion, if not all, of the *fn*-Ag nanoparticles did not undergo dissolution and were incorporated into the settled biosolids.

Ionic silver was 8–10% of the total silver in the *fn*-Ag stock solution. Therefore, the fate of ionic silver was investigated in a separate SBR operated similarly to that for *fn*-Ag. The biomass concentration over the 27-day experiment averaged 1.8 ± 0.2 mgTSS/L (Fig. SI.5). Ionic silver at these loadings in our SBR had little detrimental effects on COD removal or TSS levels (Figs. SI.3 and SI.5). The average silver removal was $94 \pm 3\%$; the influent ionic silver concentration was 0.90 ± 0.03 mg/L. Ionic silver readily sorbs to wastewater biomass [39]. However, in control experiments (no biomass) with ionic silver, silver was removed from the supernatant, which suggests that precipitation of ionic silver could have occurred. The feed solution contained 0.25 mM chloride. Silver chloride is highly insoluble ($K_{sp} = 1.56 \times 10^{-10}$), and the predicted silver ion

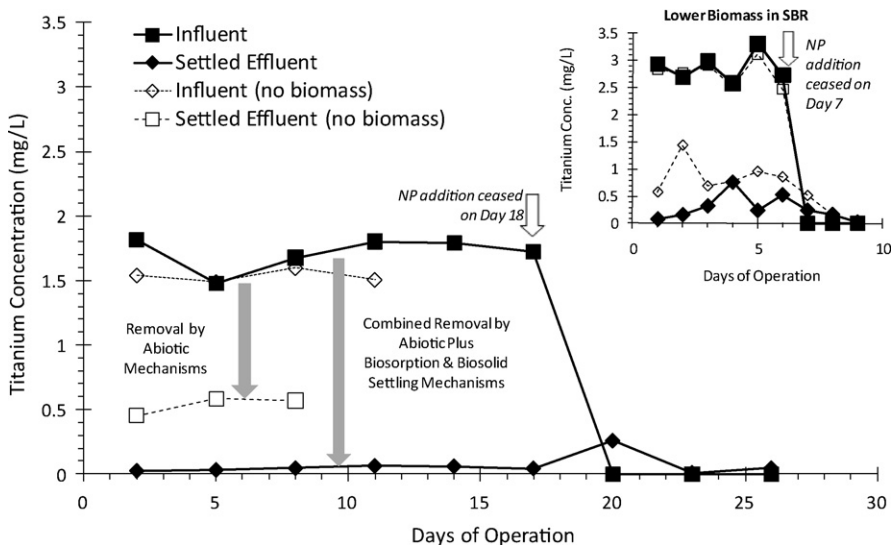


Fig. 2. Titanium concentrations in SBRs either without biomass (control, open symbols) or with biomass (solid symbols; biomass concentration ranged from 1.5 to 2.0 mgTSS/L). Inset shows results for control (no biomass) and short-term (9-day) experiments (solid symbols; biomass concentration ranged from 1.2 to 1.5 mgTSS/L).

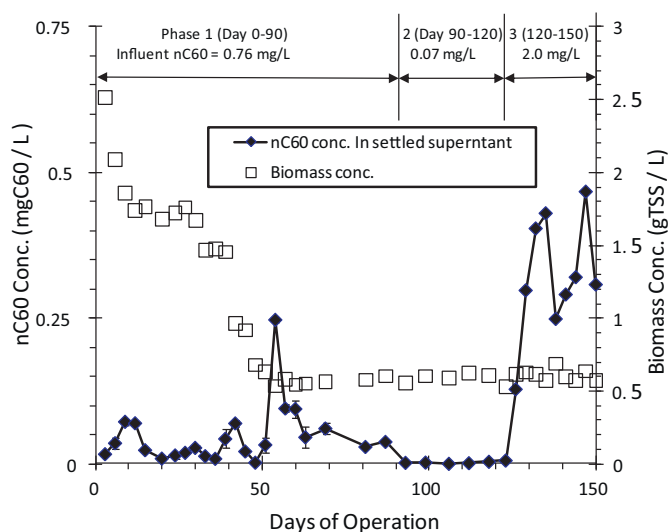


Fig. 3. Variation of nC_{60} concentration in settled supernatant during long-term operation of the SBR. During Phase 1 the influent nC_{60} was maintained at 0.764 mg/L and biomass concentration intentionally decreased. During Phases 2 and 3 the biomass concentration was maintained at a low level and nC_{60} intentionally varied.

concentration in the feed solution at equilibrium would be no more than 0.065 mgAg/L.

Fig. 2 shows the influent and effluent titanium concentrations for addition of TiO_2 to SBRs. The removal of titanium increased from 65% in the absence of biomass to $97 \pm 1\%$ with biomass present (1.3 ± 0.2 mgTSS/L). Experiments were not conducted with ionic titanium because of its extremely low solubility.

Initial experiments using fullerenes and fullerene were conducted for 6 days of NM loading plus 3 days for washout, and the NM concentrations were quantified by absorption spectroscopy. Fullerol removal determination was based upon absorbance measurements at 400 nm. Influent solutions containing fullerols had an average absorbance of $0.0447 \pm 0.0009 \text{ cm}^{-1}$. The settled effluent had an absorbance of $0.0114 \pm 0.0037 \text{ cm}^{-1}$, which equates to roughly 75% fullerol removal. On the basis of an influent fullerene concentration of ~ 2 mg/L (absorbance at 347 nm of $0.0687 \pm 0.0011 \text{ cm}^{-1}$), the settled effluent consistently contained less than 5% of the influent concentration (i.e., >95% removal). Quantification of higher removals was complicated by the presence in the settled effluent of organics that also had absorbance at 347 nm. The Day 6 sample underwent solid phase extraction and LC/MS following methods outlined elsewhere [40]; this analysis suggested that very low concentrations of fullerenes were present (<0.1 mg/L, which equates to >95% removal). However, extraction and low-level quantification is more difficult for fullerols than for nC_{60} and was not undertaken here [41].

To document the long-term and variable operation of SBRs, continuous daily nC_{60} loading into a SBR was conducted over nearly 5 months. Biomass concentrations and nC_{60} loadings were intentionally varied (Fig. 3). The influent nC_{60} concentration was 0.76 mg/L during Phase 1 (Days 0–90). During the first 30 days the biomass concentration was maintained at 1.8–2.2 g/L, and the nC_{60} concentration in the settled supernatant averaged 0.03 mg/L (96% removal). The biomass concentration was then gradually decreased to 0.6 g/L by Day 60 by supplying less carbon substrate (COD = 500 mg/L) and reducing the SRT from 6.4 days to 4.4 days. From Days 60 to 90 the nC_{60} concentration in the settled supernatant averaged 0.06 mg/L (92% removal). Despite the 70% decrease in biomass, high removals of nC_{60} persisted. During Phase 2 (Days 90–120) the influent nC_{60} concentration was reduced by a factor of 10–0.07 mg/L while maintaining the biomass concentration at

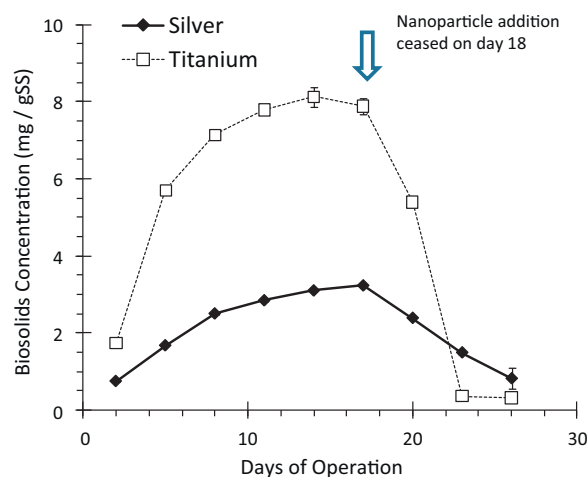


Fig. 4. Change in silver or titanium biosolid concentrations during NM loading (Days 0–18) and after cessation of NM loading (after Day 18) in the SBR.

0.6 g/L. The nC_{60} concentration in the settled supernatant averaged 0.002 mg/L (97% removal). During Phase 3 (Days 120–150) the influent nC_{60} concentration was increased to 2.0 mg/L while maintaining the same biomass (0.6 g/L). The nC_{60} concentration in the settled supernatant averaged 0.35 mg/L (83% removal). These experiments indicate excellent removal of nC_{60} under typical activated sludge biomass concentrations (>1.5 g/L), although some nC_{60} was always detectable in the settled supernatant (i.e., simulated WWTP effluent). Under very low biomass conditions and very high nC_{60} loadings (e.g., Phase 3), fullerene removal began to deteriorate.

3.3. Nanomaterial accumulation in biosolids and mass balance

Biosolid samples were collected from the SBRs once per day to manage the SRT. These samples were collected at the end of each complete mixing and aeration period (i.e., mixed liquor), prior to the settling period. The presence of NMs in biosolids was confirmed by TEM-EDX or SEM-EDX analysis (Figs. S1.8 and S1.9). Clusters of aggregated $n-TiO_2$ with a size of several hundred nanometers were present in the biosolids. In contrast, individual 1- to 20-nm silver NMs were observed in the biosolids after application of $fn-Ag$. On the basis of TEM analysis, the silver present in the biosolids had a similar size, morphology, and crystalline structure as the $fn-Ag$ applied, suggesting that the NMs largely were not transformed but rather sorbed to the biosolids. Most of the silver and titanium dioxide remained in nanoparticle form.

Silver and titanium concentrations in aggregated biosolid samples from the 27-day SBR tests are presented in Fig. 4. The data initially showed a gradual increase in the total metal (Ag or Ti) concentration in the biosolids, which began to plateau after 15–18 days of SBR operation, approximately three times the SRT value of 6.4 days. After reaching the plateau the biosolids contained approximately 3 mgAg/gSS and 8 mgTi/gSS, respectively; that is, the titanium concentrations were roughly 2.5 times higher than the silver concentrations. This is consistent with the higher removal of titanium (1.7 mgTi/L) compared with silver (0.7 mgAg/L) observed in the SBR (Figs. 1 and 2); approximately 2.4 times more titanium than silver was removed.

To demonstrate that the bioreactors would reach a steady-state NM concentration in the biomass, an SBR was operated continuously for 30 days with a fresh $fn-Ag$ loading of 2 mgAg/L in each cycle. The silver concentration in the biomass (Fig. S1.10) reached a plateau at ~ 9 mgAg/mgTSS after 10 days. SBRs must be operated for several SRTs to reach equilibrium because new biomass is

growing and because biomass is physically removed from the reactors (to control the SRT). New biomass may adsorb the NMs, thus increasing the concentration of silver in the biosolids, whereas the removal of biomass will decrease it. This increase and decrease may reach equilibrium after a sufficient period of operation. The two *fn*-Ag experiments with 2 mgAg/L (Figs. SI.7 and SI.10) resulted in roughly 3 times higher silver concentration in the biosolids than the 0.8 mgAg/L (Figs. 1 and 4), which shows that higher silver loadings lead to higher steady state biosolids concentrations of silver; the 2 mgAg/L experiment was operated at a slightly lower steady state biomass concentration (0.6 mgTSS/L; Fig. SI.7) than the 0.8 mgAg/L experiment (1.8 ± 0.2 mgTSS/L; Fig. SI.7) which accounts for the slightly higher silver concentration in the higher silver loading experiment. Overall, the results implied that short-term operation of SBR reactors (i.e., less than 2–3 times the SRT value), or even batch isotherm tests, may not accurately represent the accumulation of NMs in biosolids in a real WWTP.

Combining data for NM concentrations in settled effluent with mixed liquor samples allowed for NM mass balances to be conducted. Over the course of the SBR experiments, mass balances between metal loading and measured metal concentrations were in good agreement (<10% difference). Several mass balance plots are presented in Fig. SI.11. Closure of the mass balances is important because it confirms that other NM loss mechanisms, such as NM sorption to the reactor or attachment to bubbles (i.e., aerosolization), were negligible in the SBRs.

Overall, the data collected indicate that biological wastewater treatment plants operated using suspended biomass (e.g., activated sludge) have the potential to remove engineered nanomaterials from wastewaters. Both small, negatively charged NMs (e.g., *fn*-Ag) and larger aggregates of NMs (e.g., *n*-TiO₂) are removed by interaction with biomass in systems operated with TSS similar to that of full-scale WWTPs. The mechanisms of these interactions between NMs and bacteria appear to involve electrostatic attraction and to be size dependent [42,43]. It is apparent that in our SBRs and other batch experiments that higher biomass (TSS) concentrations improved NM removal [44]. Thus, systems operated with even higher TSS levels than those selected here, which represent common activated sludge systems, could be expected to remove NMs more efficiently. For example, membrane bioreactors (MBRs) often operate with biomass concentrations on the order of 10 gTSS/L. In addition to operating at higher biomass concentrations, the 0.1–0.4- μ m membrane employed by MBR systems would likely improve overall silver removal compared with sedimentation alone. Many older or smaller WWTPs employ fixed-film biological reactors (e.g., trickling filters) rather than the suspended biomass systems simulated here, which are used by activated sludge systems. Further research into NM removal by attached microbial communities is therefore needed.

As NM removal from wastewater occurs, NMs become concentrated in biosolids. Roughly 6–8 million tons of municipal waste biosolids are produced annually in the USA [45], and this amount is increasing because of the commissioning of new plants and upgrades of existing facilities [46]. Approximately 60% of the biosolids in the USA are applied to land, 22% incinerated, and 17% landfilled [45], but the trends are regionally variable. There is considerable debate about the proper disposal for biosolids [47]. On one hand, land application of biosolids is viewed as a sustainable practice because they provide valuable nutrients and structure to soils. On the other hand, new or more stringent regulations due to a wide array of pollutant could lead to less land application of biosolids and higher rates of incineration [47]. Incineration can recover thermal energy, but it creates new problems associated with particulate emissions and deposition of ashes into landfills. Incineration of biosolids generates particulates containing heavy metals or polyaromatic hydrocarbons [48,49]. Fly ash is often mixed

with biosolids and land applied as a fertilizer [50]. Elements used in NMs (e.g., Ti, Zn) are found in fly ash in concentrations exceeding 3000 ppm [51], but little work has characterized the mineralogy of these residuals. Approximately 170 incinerators treat biosolids within the USA [52] incinerating almost a quarter of biosolids generated in the nation [53]. Incineration is more prevalent in countries with high population density (e.g., the European Union and Japan) where land disposal is not an option or public concern about food chain contamination exists [47,51,54,55]. Additional research is needed to understand the long-term fate of NMs as biosolids are subsequently disposed.

Acknowledgements

Although the research described in the present study has been funded in part by the U.S. Environmental Protection Agency through a grant/cooperative agreement (RD831713 and RD833322), it has not been subjected to the Agency's required peer and policy review. Therefore, it does not necessarily reflect the views of the Agency, and no official endorsement should be inferred. Additional funding was provided by Water Environment Research Foundation.

Appendix A. Supplementary data

Supplementary data associated with this article can be found, in the online version, at doi:10.1016/j.jhazmat.2011.10.086.

References

- [1] A.D. Maynard, R.J. Aitken, T. Butz, V. Colvin, K. Donaldson, G. Oberdorster, M.A. Philbert, J. Ryan, A. Seaton, V. Stone, S.S. Tinkle, L. Tran, N.J. Walker, D.B. Warheit, Safe handling of nanotechnology, *Nature* 444 (2006) 267–269.
- [2] Woodrow Wilson, The project on emerging technologies. <<http://www.nanotechproject.org/>>, 2009.
- [3] M. Muhling, A. Bradford, J.W. Readman, P.J. Somerfield, R.D. Handy, An investigation into the effects of silver nanoparticles on antibiotic resistance of naturally occurring bacteria in an estuarine sediment, *Mar. Environ. Res.* 68 (2009) 278–283.
- [4] C.S. Ramsden, T.J. Smith, B.J. Shaw, R.D. Handy, Dietary exposure to titanium dioxide nanoparticles in rainbow trout, (*Oncorhynchus mykiss*): no effect on growth, but subtle biochemical disturbances in the brain, *Ecotoxicology* 18 (2009) 939–951.
- [5] R.D. Handy, A.N. Jha, A. Al-Jubory, In vitro techniques and their application to nanoparticles, *Comp. Biochem. Physiol. A: Mol. Integr. Physiol.* 153A (2009), S87–S87.
- [6] G. Oberdorster, V. Stone, K. Donaldson, Toxicology of nanoparticles: a historical perspective, *Nanotoxicology* 1 (2007) 2–25.
- [7] S.J. Klaine, P.J.J. Alvarez, G.E. Batley, T.F. Fernandes, R.D. Handy, D.Y. Lyon, S. Mahendra, M.J. McLaughlin, J.R. Lead, Nanomaterials in the environment: behavior, fate, bioavailability, and effects, *Environ. Toxicol. Chem.* 27 (2008) 1825–1851.
- [8] R.D. Handy, R. Owen, E. Valsami-Jones, The ecotoxicology of nanoparticles and nanomaterials: current status, knowledge gaps, challenges, and future needs, *Ecotoxicology* 17 (2008) 315–325.
- [9] N. Duran, P.D. Marcato, G.I.H. De Souza, O.L. Alves, E. Esposito, Antibacterial effect of silver nanoparticles produced by fungal process on textile fabrics and their effluent treatment, *J. Biomed. Nanotechnol.* 3 (2007) 203–208.
- [10] Z.H. Tong, M. Bischoff, L. Nies, B. Applegate, R.F. Turco, Impact of fullerene (C-60) on a soil microbial community, *Environ. Sci. Technol.* 41 (2007) 2985–2991.
- [11] J.P. Cheng, E. Flahaut, S.H. Cheng, Effect of carbon nanotubes on developing zebrafish (*Danio rerio*) embryos, *Environ. Toxicol. Chem.* 26 (2007) 708–716.
- [12] M.N. Moore, Do nanoparticles present ecotoxicological risks for the health of the aquatic environment? *Environ. Int.* 32 (2006) 967–976.
- [13] E. Oberdorster, S.Q. Zhu, T.M. Blickey, P. McClellan-Green, M.L. Haasch, Ecotoxicology of carbon-based engineered nanoparticles: effects of fullerene (C-60) on aquatic organisms, *Carbon* 44 (2006) 1112–1120.
- [14] C.O. Robichaud, A. Uyar, M.R. Darby, L.G. Zucker, M. Wiesner, Estimates of upper bounds and trends in nano-TiO₂ production as a basis for exposure assessment, *Environ. Sci. Technol.* 43 (12) (2009) 4227–4233.
- [15] M.R. Wiesner, G.V. Lowry, K.L. Jones, M.F. Hochella, R.T. Di Giulio, E. Casman, E.S. Bernhardt, Decreasing Uncertainties in Assessing Environmental Exposure, Risk, and Ecological Implications of Nanomaterials, *Environ. Sci. Technol.* 43 (2009) 6458–6462.
- [16] B. Nowack, Is anything out there? What life cycle perspectives of nano-products can tell us about nanoparticles in the environment, *Nano Today* 4 (2009) 11–12.

- [17] F. Gottschalk, T. Sonderer, R.W. Scholz, B. Nowack, Modeled environmental concentrations of engineered nanomaterials (TiO₂, ZnO, Ag, CNT, fullerenes) for different regions, *Environ. Sci. Technol.* 43 (2009) 9216–9222.
- [18] N.C. Mueller, B. Nowack, Exposure modeling of engineered nanoparticles in the environment, *Environ. Sci. Technol.* 42 (2008) 4447–4453.
- [19] B. Nowack, T.D. Bucheli, Occurrence, behavior and effects of nanoparticles in the environment, *Environ. Pollut.* 150 (2007) 5–22.
- [20] B. Nowack, The behavior and effects of nanoparticles in the environment, *Environ. Pollut.* 157 (2009) 1063–1064.
- [21] M. S.K.V. Brar, R.D. Tyagi, R.Y. Surampalli, Engineered nanoparticles in wastewater and wastewater sludge—evidence and impacts, *Waste Manage.* 30 (2010) 504–520.
- [22] L. Nyberg, R.F. Turco, L. Nies, Assessing the impact of nanomaterials on anaerobic microbial communities, *Environ. Sci. Technol.* 42 (2008) 1938–1943.
- [23] M.A. Kiser, P. Westerhoff, T. Benn, Y. Wang, J. Perez-Rivera, K. Hristovski, Titanium nanomaterial removal and release from wastewater treatment plants, *Environ. Sci. Technol.* (2009).
- [24] T. Benn, The Release of Engineered Nanomaterials from Commercial Products, School of Sustainable Engineering and The Built Environment, Arizona State University, Tempe, AZ, 2009.
- [25] L.K. Limbach, R. Bereiter, E. Mueller, R. Krebs, R. Gaelli, W.J. Stark, Removal of oxide nanoparticles in a model wastewater treatment plant: influence of agglomeration and surfactants on clearing efficiency, *Environ. Sci. Technol.* 42 (2008) 5828–5833.
- [26] B. Kim, C.S. Park, M. Murayama, M.F. Hochella, Discovery and characterization of silver sulfide nanoparticles in final sewage sludge products, *Environ. Sci. Technol.* 44 (2010) 7509–7514.
- [27] B. Nowack, T.D. Bucheli, Occurrence, behavior and effects of nanoparticles in the environment, *Environ. Pollut.* (2007) 5–22.
- [28] Y.X. Yin, X.Q. Zhang, J. Graham, L. Luong, Examination of purified single-walled carbon nanotubes on activated sludge process using batch reactors, *J. Environ. Sci. Health A: Tox. Hazard. Subst. Environ. Eng.* 44 (2009) 661–665.
- [29] H.P. Jarvie, H. Al-Obaidi, S.M. King, M.J. Bowes, M.J. Lawrence, A.F. Drake, M.A. Green, P.J. Dobson, Fate of silica nanoparticles in simulated primary wastewater treatment, *Environ. Sci. Technol.* 43 (2009) 8622–8628.
- [30] L.K. Limbach, R. Bereiter, E. Mueller, R. Krebs, R. Gaelli, W.J. Stark, Removal of oxide nanoparticles in a model wastewater treatment plant: influence of agglomeration and surfactants on clearing efficiency, *Environ. Sci. Technol.* (2008) 5828–5833.
- [31] M.S. Moussa, C.M. Hooijmans, H.J. Lubberding, H.J. Gijzen, M.C.M. van Loosdrecht, Modelling nitrification, heterotrophic growth and predation in activated sludge, *Water Res.* 39 (2005) 5080–5098.
- [32] APHA, AWWA, WEF, Standard Methods for the Examination of Water And Wastewater (21st Edition), 20th ed., American Public Health Association, Washington, DC, 2005.
- [33] T. Benn, P. Westerhoff, P. Herckes, Detection of fullerenes (C₆₀ and C₇₀) in commercial cosmetics, *Environ. Eng. Sci.* 39 (2010) 1875–1882.
- [34] B.F. Pycke, T. Benn, P. Westerhoff, R.U. Halden, Strategies for quantifying C₆₀ fullerenes in biological samples and implications for toxicological studies, *Trends Anal. Chem.* 30 (2011) 44–57.
- [35] T.M. Benn, B.F.G. Pycke, P. Herckes, P. Westerhoff, R.U. Halden, Evaluation of extraction methods for the quantification of aqueous fullerenes in urine, *Anal. Bioanal. Chem.* 399 (4) (2011) 1631–1639.
- [36] N. Duran, P.D. Marcato, G.I.H. De Souza, O.L. Alves, E. Esposito, Antibacterial effect of silver nanoparticles produced by fungal process on textile fabrics and their effluent treatment, *J. Biomed. Nanotechnol.* (2007) 203–208.
- [37] O.K. Choi, Z.Q. Hu, Nitrification inhibition by silver nanoparticles, *Water Sci. Technol.* 59 (2009) 1669–1702.
- [38] Y. Zhang, Y. Chen, P. Westerhoff, J.C. Crittenden, Impact of natural organic matter and divalent cations on the stability of aqueous nanoparticles, *Water Res.* 43 (2009) 4249–4257.
- [39] N.W.H. Adams, J.R. Kramer, Silver speciation in wastewater effluent, surface waters, and pore waters, *Environ. Toxicol. Chem.* 18 (1999) 2667–2673.
- [40] Z. Chen, P. Westerhoff, P. Herckes, Quantification of C-60 fullerene concentrations in water, *Environ. Toxicol. Chem.* 27 (2008) 1852–1859.
- [41] T.-C. Chao, G. Song, N. Hansmeier, P. Westerhoff, P. Herckes, R.U. Halden, Characterization and LC-MS/MS based quantification of hydroxylated fullerenes, *Anal. Chem.* 83 (5) (2011) 1777–1783.
- [42] W. Zhang, A.G. Stack, Y.S. Chen, Interaction force measurement between *E. coli* cells and nanoparticles immobilized surfaces by using AFM, *Colloids Surf. B: Biointerfaces* 82 (2011) 316–324.
- [43] W. Zhang, M. Kalive, D.G. Capco, Y.S. Chen, Adsorption of hematite nanoparticles onto Caco-2 cells and the cellular impairments: effect of particle size, *Nanotechnology* 21 (2011).
- [44] M.A. Kiser, P. Westerhoff, T. Benn, Y. Wang, J. Perez-Rivera, K. Hristovski, Titanium nanomaterial removal and release from wastewater treatment plants, *Environ. Sci. Technol.* (2009) 6757–6763.
- [45] J. Peccia, T. Paez-Rubio, Quantification of airborne biological contaminants associated with land applied biosolids, final report, *Water Environ. Res. Found.* (2006) p169.
- [46] NRC, in: NRC (Ed.), *Biosolids Applied to Land: Advancing Standards and Practices*, National Academy Press, Washington, DC, 2002, p. 284.
- [47] H.L. Wang, S.L. Brown, G.N. Magesan, A.H. Slade, M. Quintern, P.W. Clinton, T.W. Payn, Technological options for the management of biosolids, *Environ. Sci. Pollut. Res.* 15 (2008) 308–317.
- [48] J.G. Shao, R. Yan, H.P. Chen, H.P. Yang, D.H. Lee, D.T. Liang, Emission characteristics of heavy metals and organic pollutants from the combustion of sewage sludge in a fluidized bed combustor, *Energy Fuels* 22 (2008) 2278–2283.
- [49] A.V. de Velden, R. Dewil, J. Baeyens, L. Jossion, P. Lanssens, The distribution of heavy metals during fluidized bed combustion of sludge (FBSC), *J. Hazard. Mater.* 151 (2008) 96–102.
- [50] L. Reijnders, Disposal, uses and treatments of combustion ashes: a review, *Resour. Conserv. Recycl.* 43 (2005) 313–336.
- [51] D. Marani, C.M. Braguglia, G. Mininni, F. Maccioni, Behaviour of Cd, Cr, Mn, Ni, Pb, and Zn in sewage sludge incineration by fluidised bed furnace, *Waste Manage.* 23 (2003) 117–124.
- [52] U. EPA, AP 42: Compilation of Air Pollutant Emission Factors, Volume 1: Stationary Point and Area Sources, 5th ed. Available from: <http://www.epa.gov/ttnchie1/ap42/> (accessed 16.01.09).
- [53] USEPA, *Biosolids Generation, Use, and Disposal in the United States*, Washington DC, 1999.
- [54] E. Commission, *Pollutants in Urban Wastewater and Sewage Sludge. Final Report*, Office for Official Publications of the European Communities, Luxembourg, 2001.
- [55] K. Hara, T. Mino, Environmental assessment of sewage sludge recycling options and treatment processes in Tokyo, *Waste Manage.* 28 (2008) 2645–2652.